AIAA JOURNAL
Vol. 44, No. 12, December 2006

Microcracking in Cross-Ply Laminates due to Biaxial Mechanical and Thermal Loading

Satish K. Bapanapalli* and Bhavani V. Sankar†
University of Florida, Gainesville, Florida 32611-6250
and
Robert J. Primas‡
Structures Technology-Advanced Analysis, Canoga Park, California 91309-7922

DOI: 10.2514/1.20798

This paper presents a methodology to predict microcracking and microcrack density in both surface and internal plies of a symmetric cross-ply laminate under biaxial mechanical and thermal loading conditions. The thermoelastic properties of the microcracked laminates at different crack densities were determined by finite element analysis of the unit cells bounded by the microcracks. Analytical expressions for the stiffness and coefficients of thermal expansion as functions of crack densities were obtained in the form of response surface approximations. These analytical expressions were then used to predict the formation of a new set of microcracks by equating the change in strain energy in the unit cell before and after the formation of the microcracks to the critical fracture energy required for their formation. Analytical expressions obtained as response surface approximations were also used to predict progressive microcracking. Both displacement and load control cases were considered along with thermal loading. Results from the current methodology agree very well with published data.

Nomenclature

$[A]$	=	2×2 laminate stiffness matrix
$[A_1]$, $[A_2]$	=	2×2 laminate stiffness matrix before and after formation of the next microcracks
$[\bar{A}]$	=	inverse of the 2×2 laminate stiffness matrix
$[\bar{A}_1]$, $[\bar{A}_2]$	=	inverses of the 2×2 laminate stiffness matrix before and after formation of the next microcracks
G_m	=	strain energy release rate for the formation of next microcrack
G_{mc}	=	microcracking fracture toughness
N_{els}	=	number of elements in the FE model
N_L	=	number of layers in the laminate
N_x, N_y	=	applied laminate stress resultants in x and y directions
$\{N\}$	=	2×1 force resultant vector
$\{N_t\}$	=	2×1 thermal force vector
$\lfloor \bar{Q}^{(k)} \rfloor$	=	2×2 stiffness matrix of the kth ply in the laminate
t	=	thickness of the laminate
t_k	=	thickness of kth ply in the laminate
t_0, t_{90}	=	thickness of the 0 and 90 deg plies
t_1, t_2	=	thicknesses of 0 and 90 deg layers in the cross-ply laminate
U	=	strain energy of the whole unit cell
$U_0^{(k)}$	=	strain energy density in the kth ply
V^i, V	=	volume of the ith element and volume of the whole unit cell
α	=	ratio of applied stress resultants (N_y/N_x)
$\{\alpha_{\mathrm{cr}}\}$	=	2×1 coefficients of thermal expansion (CTE) vector of the microcracked ply
$\{\alpha_0\}$, $\{\alpha_{90}\}$	=	2×1 CTE vector of the 0 and 90 deg plies
$\{\alpha^{(k)}\}$	=	2×1 CTE vector of kth ply
β	=	ratio of applied laminate strains ($\varepsilon_y/\varepsilon_x$)
ΔT	=	temperature change
$\{\varepsilon\}$	=	2×1 laminate strain vector
ε_x, ε_y	=	applied laminate strains in the x and y directions
λ, λ_x, λ_y	=	uniaxial microcrack density, and microcrack densities in x and y directions
σ_x^i, σ_y^i	=	stresses in the x–y coordinate system in the ith element

Presented as Paper 2230 at the AIAA/ASME/ASCE/AHS/ASC Structures, Structural Dynamics & Materials Conference, Austin, Texas, 14–18 April 2005; received 28 October 2005; revision received 8 June 2006; accepted for publication 15 September 2006.

*Graduate Research Assistant, Department of Mechanical and Aerospace Engineering, PO Box 116250. AIAA Student Member.
†Newton C. Ebaugh Professor, Department of Mechanical and Aerospace Engineering, PO Box 116250. AIAA Associate Fellow.
‡Associate Technical Fellow, Mail Stop 055-FA45, Boeing/Canoga Park, 6633 Canoga Avenue. AIAA Member.

I. Introduction

MATRIX microcracking is the first form of damage in composite laminates that are subjected to mechanical and/or hygrothermal loading. The immediate effect of microcracking is the deterioration of the thermomechanical properties of the laminate. Furthermore, it could lead to delamination and catastrophic damage of the structure. In some instances, cryogenic fuel tanks, microcracks, and delaminations make the laminates permeable to fluid flow. However, microcracking is not always an undesirable phenomenon. Microcracked textile composites are being studied for their use in future technologies such as transpiration cooling of rocket engine walls and turbine blades.

Matrix microcracks are present in structural composites during a major part of their life. Given the importance of structural composites in the aerospace industry today, there is a need to completely understand the microcracking phenomenon. Over the years researchers have put forward various methods to 1) determine the thermomechanical properties of microcracked laminates, and 2) predict the microcrack density as a function of applied stress. The majority of these studies were conducted on symmetric cross-ply laminates. In these laminates it has been observed that the cracks form in the internal as well as surface plies and span over the entire cross section of the plies. It is in general agreed that in cross-ply laminates the microcracks form and traverse the entire cross section of the ply instantaneously on an experimental time scale [1–3]. Comparatively, fewer studies have been carried out to study

microcracking in angle-ply laminates such as quasi-isotropic laminates ([4–6], not a complete list). In these laminates, it has been observed that the cracks do not traverse the whole ply cross section instantaneously. Thus, slow stable crack growth has to be considered. This paper, however, concentrates on microcracking in symmetric cross-ply laminates only with instantaneous unstable crack growth.

Figure 1 illustrates the formation of the next microcrack in the internal 90 deg plies of a unit cell of damage bounded by two preexisting microcracks. The laminate is designated as $[(S)/90_n]_s$ laminate, where (S) denotes a set of supporting plies which could be 0 deg or any set of off-axis plies. In the case of $[90_n/(S)]_s$ laminates, microcracks form in the surface plies. The unit cell of damage is shown in Fig. 2a. The cracks in one outer ply are staggered with respect to the other ply [3]. The next stage of cracking is shown in Fig. 2b where a single unit cell breaks up into three unit cells of damage by the formation of four new microcracks. Crack density increases by a factor of 3 to preserve the staggered pattern of microcracks. It should be noted that a unit-cell analysis implies the assumption that the distribution of cracks along the length of the laminate is uniform. Nonuniform crack spacing has also been studied by researchers. McCartney [7] proposed some simple additions to the analytical formulas for uniform crack spacing. Silberschmidt [8] concluded that, although the unit-cell analyses might lead to incorrect results, they provide useful lower and upper bounds for the minimum and maximum crack spacing in the case of nonuniform crack spacing. In the current research work, the unit-cell approach is adopted in keeping with the general trend of research in the field of microcracking.

Nairn [3] used a *finite fracture mechanics* approach to predict the formation of microcracks in the 90 deg plies. In this approach, the strain energy release rate for the formation of a new microcrack, G_m, is calculated as a function of applied stresses, mechanical properties of the composite and the microcracked laminate, and the microcrack density. This G_m is then equated to the "microcracking fracture toughness," G_{mc}, in order to solve for the stresses required to form the new microcracks. G_{mc} has been shown to be a material property and experimental techniques are available to determine the G_{mc} of a composite [3]. The strain energy release rate was shown to be different for displacement control and load control conditions. This finite fracture mechanics method predicted the progressive microcracking very well. The predictions are limited to uniaxial loading and microcrack formation in the internal or surface plies but not in both at the same time. The methodology presented in the current manuscript is, in a sense, an extension of Nairn's approach to include biaxial loading conditions which takes into account the formation of microcracks in both surface and internal plies at the same time.

McCartney [9,10] developed a generalized plane strain analytical model to predict progressive microcracking by equating the difference in strain energy before and after the formation of the microcracks to the fracture energy required to form a unit area of microcrack. This analysis considered cracking only in the internal 90 deg plies of a general symmetric laminate and not the surface plies. This model took into account triaxial loading conditions and thermal residual stresses. A statistical distribution of fracture energies in the laminate was used. Statistical models [10–14] for distribution of strength or fracture energies are closer to reality as they take into account imperfections like the variation of fiber distribution in the 90 deg layers and the inherent flaws in the composite materials. Nairn [3] suggested using a stochastic variation of microcracking fracture toughness, G_{mc}, to account for the imperfections.

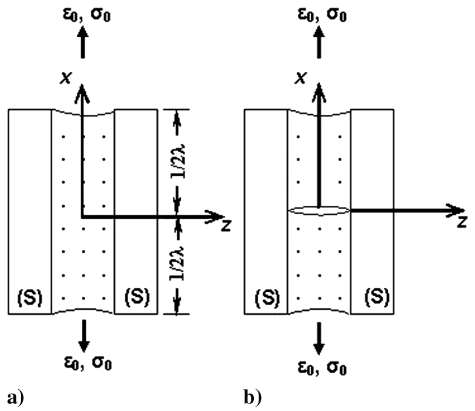

Fig. 1 a) Unit cell of damage for internal microcracks in an $[(S)/90_n]_s$ laminate; b) formation of next microcrack in the internal 90 deg ply. λ is the microcrack density.

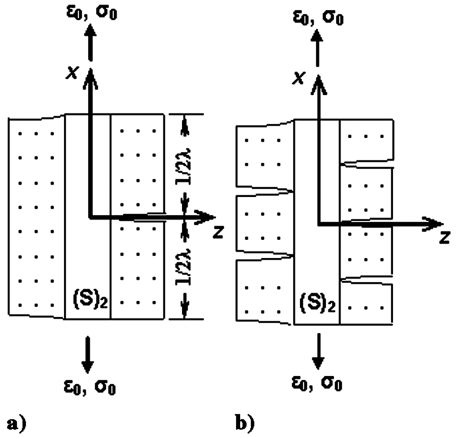

Fig. 2 a) Unit cell of damage for cracks in 90 deg on the surface; b) formation of next microcracks, which break up the unit cell into three new unit cells. λ is the microcrack density.

Early progressive microcracking models used transverse strength of a composite as a criterion for the formation of new microcracks [12,15–17]. Nairn [3], however, argues against these strength-based models because the behavior of a ply as part of a laminate is dependent on the laminate stacking sequence and is different from the conditions for transverse-strength tests. It has also been shown that the transverse-strength based model predictions for progressive microcracking are not consistent with experimental observations.

To predict progressive microcracking, it is essential to have an accurate model to determine the thermomechanical properties of the microcracked laminate. Shear lag methods [17–20] are the most popular analytical techniques to predict the properties. Variational methods introduced by Hashin [21] and extended by Nairn [22,23] have also been shown to be good when compared with the experimental data. Average crack opening displacement (COD) has been used by some researchers as a parameter to express modulus and energy release rate [24–27]. Finite element (FE) analysis has been used to predict the thermomechanical properties of microcracked laminates [20,28]. Berthelot [29] compares the finite element analysis with other analytical techniques to show that a shear lag model which uses a parabolic distribution of stresses in the thickness direction of the plies gives results that agree well with those obtained from FE analysis.

Analytical methods can be applied for microcracking in one direction. If the microcracks form in both directions, the problem would become too complicated to be treated by analytical methods. Aboudi et al. [30] present the only available analytical model that takes into account microcracking in both directions in cross-ply laminates. They present an approximate 3-D analysis to determine the stiffness and Poisson's ratio of a microcracked cross-ply laminate.

In the current research, FE analysis has been used to obtain the average thermoelastic properties of the laminate with microcracks in both directions. The key feature of this work was to obtain analytical expressions for stiffness and coefficients of thermal expansion (CTE) components, as functions of crack densities, using response surface approximations. This facilitates analytical differentiation of strain energy with respect to crack densities. Microcracking fracture toughness G_{mc} was used for the critical fracture energy release rate.

Progressive microcracking was predicted using these analytical expressions and the critical energy release rate. Both mechanical and thermal loading were considered.

II. Methodology to Predict Microcracking due to Biaxial Loading Conditions

The current research proposes a method to predict the microcrack density in both surface and internal plies, henceforth termed as "bidirectional microcracking," in symmetric cross-ply laminates subjected to biaxial mechanical and thermal loading. The composite is loaded in its principal material axis by uniform in-plane loads N_x and N_y (but without shear loads). Thermal loads combined with mechanical loads are discussed in Sec. VI. The method is similar to the finite fracture mechanics technique used by Nairn [3] in which the difference in the strain energy of a unit cell before and after the formation of the next microcrack is equated to the total energy required to form this microcrack. The unit cell for bidirectional microcracking, shown in Fig. 3 for a $[90_n/0_m]_s$ laminate, is a "combination" of the two unit cells shown in Figs. 1 and 2. The definition of crack densities is accordingly modified and denoted by λ_x and λ_y, as shown in Fig. 3.

For load control conditions, the difference in strain energy before and after the formation of the next microcrack is given by

$$G_m = \frac{1}{2}\lfloor N_x \quad N_y \rfloor \cdot ([\bar{A}_2] - [\bar{A}_1]) \cdot \{ {N_x \atop N_y} \} \cdot \frac{1}{\lambda_x} \cdot \frac{1}{\lambda_y} \tag{1}$$

where G_m is the strain energy release rate, N_x and N_y are the force resultants in the x and y directions, and λ_x and λ_y are the microcrack densities in the x and y directions. Equation (1) can be written as

$$G_m = \frac{1}{2}\lfloor N_x \quad N_y \rfloor \cdot [\Delta\bar{A}] \cdot \{ {N_x \atop N_y} \} \cdot \frac{1}{\lambda_x} \cdot \frac{1}{\lambda_y} \tag{2}$$

where $[\Delta\bar{A}] = [\bar{A}_2] - [\bar{A}_1]$. In practical situations, the force resultants (N_x and N_y) are proportional to one another. For example, in a cylindrical pressure vessel the hoop stress N_y is twice the axial stress N_x. In the case of thermal stresses, the relation between N_x and N_y is dependent on the CTEs of the laminate in the x and y directions. In general, the proportional loading relationship can be written as

$$N_y = \alpha \cdot N_x \tag{3}$$

where α is a nondimensional constant. The expression in Eq. (2) can then be simplified as

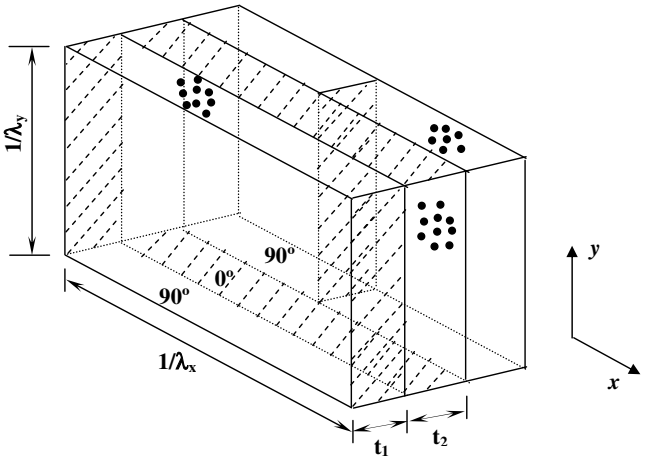

Fig. 3 Unit cell with cracks in both 0 deg (x direction) and 90 deg plies of a $[90_n/0_m]_s$ laminate. The hatched regions are the cracks' surfaces. The black dots are fiber tips visible on the surfaces. The crack density in the x direction is λ_x and in the y direction is λ_y.

$$G_m = \frac{1}{2}(\Delta A_{11} + 2\alpha\Delta A_{12} + \alpha^2\Delta A_{22}) \times N_x^2 \times \frac{1}{l_x} \times \frac{1}{l_y} \tag{4}$$

where $\Delta\bar{A}_{11} = \bar{A}_{2_{11}} - \bar{A}_{1_{11}}$, $\Delta\bar{A}_{12} = \bar{A}_{2_{12}} - \bar{A}_{1_{12}}$, and $\Delta\bar{A}_{22} = \bar{A}_{2_{11}} - \bar{A}_{1_{11}}$.

The formation of the new microcracks can happen in three different ways:

Case I: formation of microcracks in the surface plies (the crack density in the x direction becomes $3\lambda_x$ and the crack density in the y direction remains λ_y);

Case II: formation of microcracks in the internal ply (the crack density in the x direction remains λ_x and the crack density in the y direction becomes $2\lambda_y$); and

Case III: formation of microcracks in both surface and internal plies (the crack density in the x direction becomes $3\lambda_x$ and the crack density in the y direction becomes $2\lambda_y$).

In case I, four new microcracks are formed in the surface plies and the total energy ΔU required for this is

$$\Delta U = 4G_{\text{mc}}\frac{1}{\lambda_y}t_1 \tag{5}$$

where G_{mc} is the microcracking fracture toughness [3], and t_1 is the thickness of the surface plies (90 deg plies). For case II, only one microcrack forms in the internal ply of the unit cell and the energy required for this is

$$\Delta U = G_{\text{mc}}\frac{1}{\lambda_x}t_2 \tag{6}$$

where t_2 is the thickness of the internal plies (0 deg plies). For case III, the energy required is the sum of Eqs. (5) and (6),

$$\Delta U = 4G_{\text{mc}}\frac{1}{\lambda_y}t_1 + G_{\text{mc}}\frac{1}{\lambda_x}t_2 \tag{7}$$

Equating Eqs. (5–7) to Eq. (4), we can solve for N_x for different cases I–III to obtain

$$N_{x(\text{I})} = \sqrt{\frac{8G_{\text{mc}}t_1}{(\Delta\bar{A}_{11} + 2\alpha\cdot\Delta\bar{A}_{12} + \alpha^2\cdot\Delta\bar{A}_{22})\cdot\frac{1}{\lambda_x}}} \qquad \text{(CASE I)} \tag{8}$$

$$N_{x(\text{II})} = \sqrt{\frac{2G_{\text{mc}}t_2}{(\Delta\bar{A}_{11} + 2\alpha\cdot\Delta\bar{A}_{12} + \alpha^2\cdot\Delta\bar{A}_{22})\cdot\frac{1}{\lambda_y}}} \qquad \text{(CASE II)} \tag{9}$$

$$N_{x(\text{III})} = \sqrt{\frac{2[(G_{\text{mc}}\frac{1}{\lambda_x}t_2) + (4G_{\text{mc}}\frac{1}{\lambda_y}t_1)]}{(\Delta\bar{A}_{11} + 2\alpha\cdot\Delta\bar{A}_{12} + \alpha^2\cdot\Delta\bar{A}_{22})\cdot\frac{1}{\lambda_x}\cdot\frac{1}{\lambda_y}}} \qquad \text{(CASE III)} \tag{10}$$

The least among $N_{x(\text{I})}$, $N_{x(\text{II})}$, and $N_{x(\text{III})}$ will be the case that will happen. For example, if $N_{x(\text{I})}$ is the least among the three, then continued loading would cause the new microcracks to form in the surface plies (x direction).

The method described above can be extended to displacement control conditions by replacing the force resultants (N_x and N_y) with strains (ε_x and ε_y) and the $[\bar{A}]$ matrix with $[A]$. The equations for displacement control can be derived as

$$\varepsilon_{x(\text{I})} = \sqrt{\frac{8G_{\text{mc}}t_1}{(\Delta A_{11} + 2\beta\cdot\Delta A_{12} + \beta^2\cdot\Delta A_{22})\cdot\frac{1}{\lambda_x}}} \qquad \text{(CASE I)} \tag{11}$$

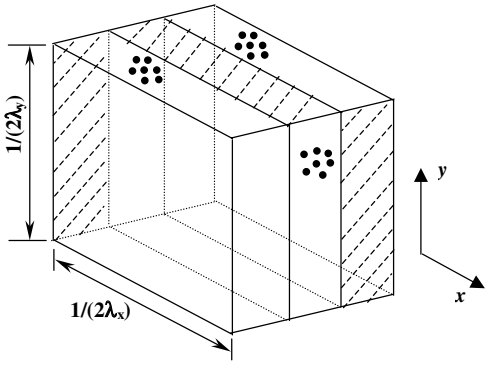

Fig. 4 One-quarter of the unit cell was used in the FE model. The hatched regions are the cracks' surfaces.

$$\varepsilon_{x(\mathrm{II})} = \sqrt{\frac{2G_{\mathrm{mc}}t_2}{(\Delta A_{11} + 2\beta\cdot\Delta A_{12} + \beta^2\cdot\Delta A_{22})\cdot\frac{1}{\lambda_y}}} \qquad \text{(CASE II)} \tag{12}$$

$$\varepsilon_{x(\mathrm{III})} = \sqrt{\frac{2[(G_{\mathrm{mc}}\frac{1}{\lambda_x}t_2) + (4G_{\mathrm{mc}}\frac{1}{\lambda_y}t_1)]}{(\Delta A_{11} + 2\beta\cdot\Delta A_{12} + \beta^2\cdot\Delta A_{22})\cdot\frac{1}{\lambda_x}\cdot\frac{1}{\lambda_y}}} \qquad \text{(CASE III)} \tag{13}$$

where $\Delta A_{11} = A_{1_{11}} - A_{2_{11}}$, $\Delta A_{12} = A_{1_{12}} - A_{2_{12}}$, $\Delta A_{22} = A_{1_{22}} - A_{2_{22}}$, and β is a nondimensional constant relating the strains in the x and y directions:

$$\varepsilon_y = \beta\cdot\varepsilon_x \tag{14}$$

III. Finite Element Method to Determine the Laminate Stiffness Matrix

The laminate stiffness matrix $[A]$ of a bidirectionally microcracked laminate was obtained by carrying out a finite element analysis of the unit cell of damage (Fig. 3). Analysis was performed on one-quarter of the unit cell, Fig. 4, by taking advantage of the symmetry. An eight node brick element (C3D8R, ABAQUS™) was used for modeling. The number of nodes and elements varied with the dimensions of the unit cell. Typically 20,000 nodes with 20,000 elements were used.

The components of the first column of the $[A]$ matrix, A_{11} and A_{21}, were obtained by imposing a unit strain in the x direction ($\varepsilon_x = 1$) and zero strain in the y direction ($\varepsilon_y = 0$) and calculating the resulting stress resultants, N_x and N_y. Unit strain in the x direction was applied by imposing a displacement of $1/2\lambda_x$ on the unhatched surfaces with normals in the positive x direction, and zero displacement in the x direction on the unhatched surfaces with normals in the negative x direction (refer to Fig. 4). Zero strain in the y direction was applied by imposing a zero displacement in the y direction on the unhatched surfaces with normals in both positive and negative y directions (Fig. 4). The elemental stresses from the FE analyses were volume averaged and multiplied by the laminate thickness to obtain the stress resultants:

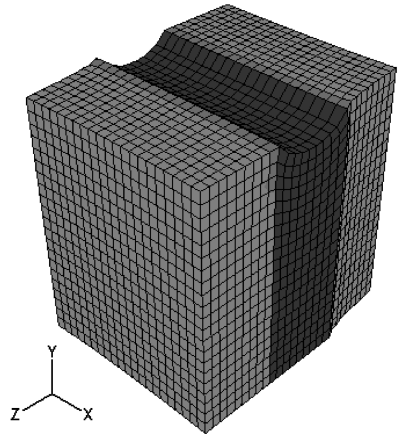

Fig. 5 Typical deformation of a unit cell ($\lambda_x = 6.3$ cracks/cm and $\lambda_y = 6.3$ cracks/cm) due to $\varepsilon_y = 1$ and $\varepsilon_x = 0$. (Deformation not to scale.)

$$N_x = \frac{\sum_i^{N_{\mathrm{els}}}\sigma_x^i V^i}{V}\cdot t \tag{15}$$

$$N_y = \frac{\sum_i^{N_{\mathrm{els}}}\sigma_y^i V^i}{V}\cdot t \tag{16}$$

Because $\varepsilon_x = 1$ and $\varepsilon_y = 0$, we have $A_{11} = N_x$ and $A_{21} = N_y$ from the following equation:

$$\begin{Bmatrix} N_x \\ N_y \end{Bmatrix} = \begin{bmatrix} A_{11} & A_{12} \\ A_{12} & A_{22} \end{bmatrix}\cdot\begin{Bmatrix} \varepsilon_x \\ \varepsilon_y \end{Bmatrix} \tag{17}$$

A similar analysis can be carried out by imposing a unit strain in the y direction and a zero strain in the x direction to obtain A_{12} and A_{22}. A typical deformation of a unit cell with a unit strain imposed in the y direction is shown in Fig. 5.

IV. Comparison of Current Methodology with Finite Fracture Mechanics Approach

The finite fracture mechanics technique used by Nairn [3] predicts the experimental results of progressive microcracking very well. Variational methods were used to derive the energy release rates for

Table 1 Orthotropic material properties for the unidirectional lamina used in the FE model

Property	Value
E_1	169 GPa (24.5 Msi)
E_2, E_3	8.62 Gpa (1.25 Msi)
ν_{12}, ν_{13}	0.355
ν_{23}	0.410
G_{12}, G_{13}	5.0 Gpa (0.73 Msi)
G_{23}	1.22 Gpa (0.177 Msi)

Table 2 Comparison of the current model results with Nairn's model. The stresses (σ) are values at which the next microcacks form in the laminate. Directions of the x and y axes can be viewed in Fig. 3

Surface cracks ($\lambda_x = 1.18$ *cracks/cm and* $\lambda_y = 0.0$ *cracks/cm*)			
Loading condition	σ_x, MPa, [3]	σ_x, MPa, current model	Difference %
Load control	416	421	1.3
Displacement control	427	428	0.2
Internal cracks ($\lambda_x = 0.0$ *cracks/cm and* $\lambda_y = 1.58$ *cracks/cm*)			
Loading condition	σ_y, MPa, [3]	σ_y, MPa, current model	Difference %
Load control	1203	1240	3.1
Displacement control	1200	1244	3.7

load and displacement control cases. In this section, the methodology presented in Sec. II is compared with Nairn's model.

A $[90_2/0]_s$ laminate (0 deg in the x direction) with a ply thickness of 0.165 mm (0.0065 in.) was used for this purpose. The orthotropic ply properties used in the FE simulations are listed in Table 1. A microcracking fracture toughness (G_{mc}) value, typical of polymer composites, of 250 J/m^2 was used. Also, only mechanically applied stresses were considered.

Results are presented in Table 2. It should be noted that Nairn's formulas are for uniaxial microcracking only. Uniaxial microcracking is a particular case of the more general bidirectional microcracking. Therefore the comparison in Table 2 is between Nairn's method and the present bidirectional microcracking method applied for the special cases of uniaxial loading. Table 2 shows excellent agreement between the two methods and hence it can be concluded that the method presented in Sec. II is comparable to Nairn's model.

V. Progressive Bidirectional Microcracking

The crucial part in the methodology presented is the determination of laminate stiffness matrix [A] for a bidirectionally microcracked laminate with arbitrary (but uniform) crack densities. With the FE simulations [A] can be determined for a particular set of microcrack densities (λ_x and λ_y). If an arbitrary set of λ_x and λ_y were chosen, one can follow the procedure shown in Sec. II to predict the loads for the formation of the next microcracks. Following this, the [A] matrix for the new set of λ_x and λ_y can be determined and proceed further till sufficiently high crack density is reached. Now, if a different set of crack densities were to be chosen to begin with, then the whole process of determining the [A] matrices for each new set has to be repeated. This is a laborious and expensive process. This is a situation wherein analytical methods to determine [A] can be very useful. However, to mitigate the tedium associated with the FE simulations as well as to take advantage of analytical methods, a novel procedure was conceived for this research.

The crack densities over a given range were considered for the purpose of simulations: λ_x in the range of 0 to 12.6 cracks/cm (0–32 cracks/in.) and λ_y in the range of 0–9.5 cracks/cm (0–24 cracks/in.). The stiffness matrices [A] for certain crack densities in this range were determined with the FE simulations. Using this data, a complete cubic polynomial in two variables, λ_x and λ_y, was fitted by a least squares approximation method for each component of the [A] matrix. Figures 6a–6c show, respectively, A_{11}, A_{12}, and A_{22} as functions of λ_x and λ_y for the $[90_2/0]_s$ laminate discussed in Sec. IV. A_{21} is equal to A_{12} for this symmetric cross-ply laminate. The surfaces in the plots are the cubic polynomial response surface approximations (in λ_x and λ_y). The 56 black dots in each plot are components of the stiffness matrices obtained from FE simulations. In this way analytical expressions were obtained for the components of [A] as a function of the crack densities.

The expressions for A_{11}, A_{12}, and A_{22} and Eqs. (8–10) for load control were used as input to a MATLAB program. The MATLAB program requires an input of initial crack densities, λ_x and λ_y. It then calculates $N_{x(I)}$, $N_{x(II)}$, and $N_{x(III)}$ [using Eqs. (8–10)] and determines the least among the three values. Thus the formation of the next microcrack is determined. The crack densities are updated accordingly, and the new laminate stiffness matrices are obtained by using the analytical expressions for A_{11}, A_{12}, and A_{22}. This procedure for progressive bidirectional microcracking is repeated until one of the crack densities exceeds the upper bound (12.6 cracks/cm for λ_x and 9.5 cracks/cm for λ_y). Progressive microcracking depends on the initial crack densities. Different initial crack densities were input to the program and the progressive microcracking was plotted as a function of applied stress as shown in Fig. 7a. The value of α [Eq. (3)] was chosen as 2.0 to simulate the stresses in a thin shell cylindrical pressure vessel with the x axis in the axial direction and the y axis in the circumferential direction. For example, consider the case of densities $\lambda_x = 0.14$ cracks/cm (curve 5 shown as a "dashed x" line) and $\lambda_y = 0.14$ cracks/cm (curve 6 shown as a "dashed +" line). Initially the cracks start to form

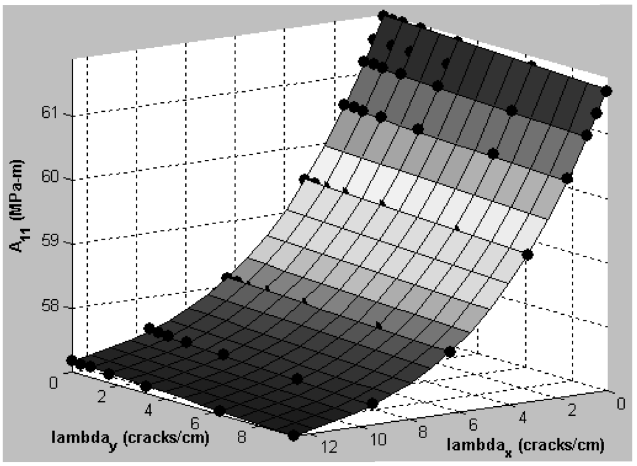

a)

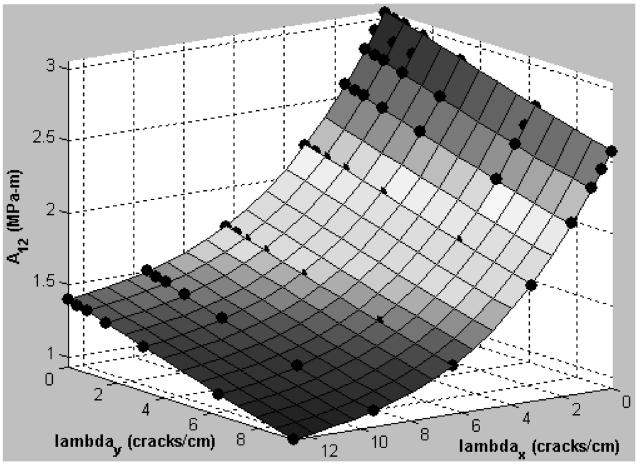

b)

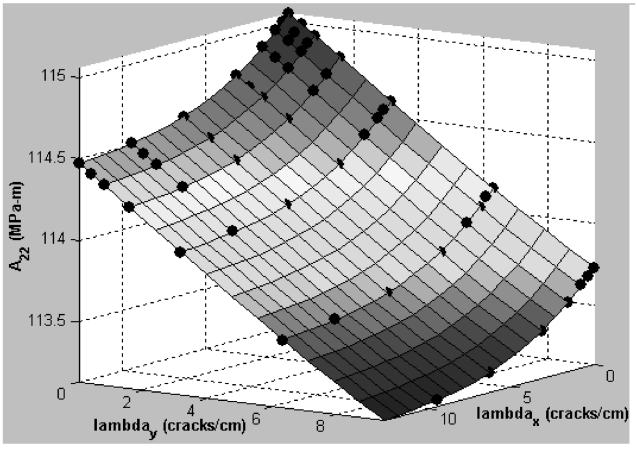

c)

Fig. 6 Complete cubic polynomial fit using least squares approximation over 56 data points (black dots) obtained from FE simulations. a) A_{11}, b) A_{12}, and c) A_{22}.

in the x direction and λ_x increases to 3.72 cracks/cm, while λ_y remains constant. After this, the stress required for the formation of microcracks in the x direction is higher than that for microcracking in the y direction. Therefore, λ_y starts to increase while λ_x remains constant. The information from Fig. 7a, for different initial crack densities, was used to obtain the progressive bidirectional microcracking as a function of applied stress (resultants), as shown in Fig. 7b. The figure shows that the microcracking in the surface plies begins at a lower stress than for the internal plies for this

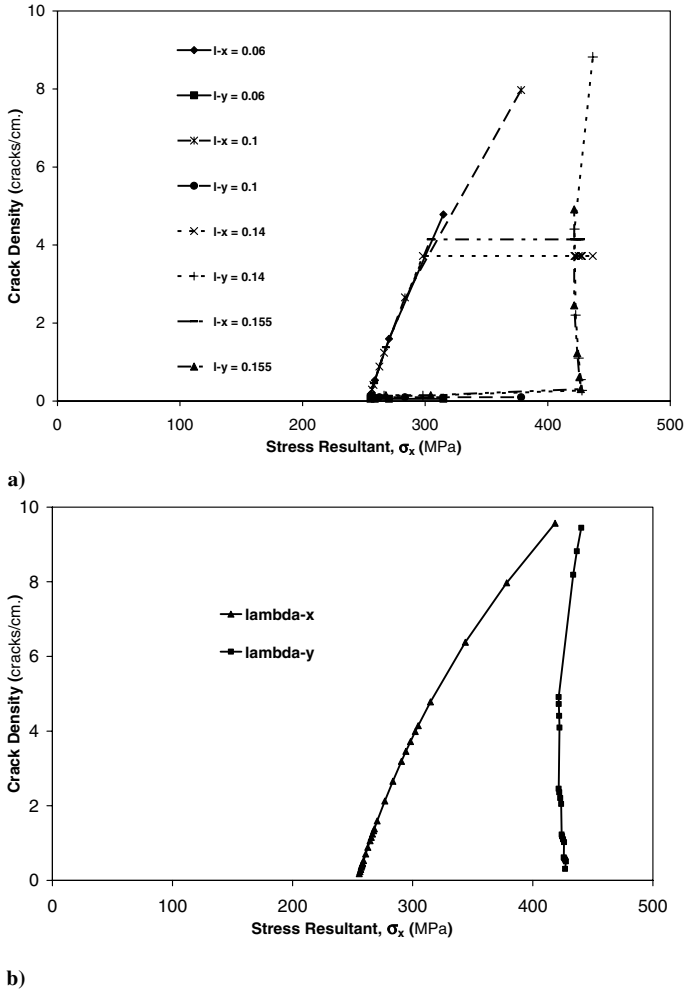

Fig. 7 a) Progressive bidirectional microcracking for different initial crack densities. In the legend, "l-x" and "l-y" stand for λ_x and λ_y and the numbers in the legend are initial crack densities. b) Crack densities as a function of applied stress (resultant). For both plots, $N_y/N_x = 2.0$. All the points in a) were combined to obtain plot b).

particular case of biaxial loading. The curve for λ_y has a negative slope in the beginning, which means that these high-density microcracks will appear instantaneously when the load reaches a critical value. It should be pointed out that a similar negative slope can be observed for microcracking in surface plies of this type of laminate in [3].

VI. Effect of Thermal Stresses

In cross-ply polymer composite laminates, thermal stresses can be significant enough to cause microcracking. Advanced composites are processed at temperatures in the range of 180°C (355°F), and when cooled down to room temperature, the resulting thermal stresses could produce microcracking in both surface and internal plies. Thus a laminate could have microcracks even before it is subjected to mechanical loads. Laminates subjected to cryogenic conditions and cyclic thermal loading exhibit significant microcracking even before they are mechanically loaded [31–34].

In the Appendix, the strain energy in a unit cell for load control conditions in the presence of thermal stresses is derived as

$$U = \left(\frac{1}{2}\{N\}^T[\bar{A}]\{N\} - \frac{1}{2}\{N_t\}^T[\bar{A}]\{N_t\} + \sum_{k=1}^{NL}\frac{1}{2}\{\alpha^{(k)}\}^T[\bar{Q}^{(k)}]\{\alpha^{(k)}\}\cdot\Delta T^2 t_k\right)\cdot\frac{1}{\lambda_x}\cdot\frac{1}{\lambda_y} \tag{18}$$

and for displacement control conditions as

$$U = \left(\frac{1}{2}\{\varepsilon\}^T[A]\{\varepsilon\} - \{\varepsilon\}^T\{N_t\} + \sum_{k=1}^{NL}\frac{1}{2}\{\alpha^{(k)}\}^T[\bar{Q}^{(k)}]\{\alpha^{(k)}\}\cdot\Delta T^2 t_k\right)\cdot\frac{1}{\lambda_x}\cdot\frac{1}{\lambda_y} \tag{19}$$

where $\{N\}$ and $\{\varepsilon\}$ are the 2×1 vectors of applied stress resultants and strains, respectively, $[\bar{Q}^{(k)}]$ is the 2×2 stiffness matrix of the kth layer, $\{\alpha^{(k)}\}$ is the 2×1 vector of CTEs of the kth layer, t_k is the thickness of the kth layer, ΔT is the temperature difference with respect to the stress free temperature, and $\{N_t\}$ is the 2×1 thermal force vector [defined in the Appendix, Eq. (A4) and reproduced here],

$$\{N_t\} = \sum_{k=1}^{NL}[\bar{Q}^{(k)}]\{\alpha^{(k)}\}\cdot t_k\Delta T \tag{20}$$

By normalizing the thermal force in Eq. (20) with ΔT we obtained a new quantity, $\{N_t'\}$, which is a laminate property.

$$\{N_t'\} = \sum_{k=1}^{NL}[\bar{Q}^{(k)}]\{\alpha^{(k)}\}\cdot t_k \tag{21}$$

Similarly we can define a new quantity U', by dividing the last term in the parentheses in Eqs. (18) and (19) with ΔT^2:

$$U' = \sum_{k=1}^{NL} \frac{1}{2} \{\alpha^{(k)}\}^T [\bar{Q}^{(k)}] \{\alpha^{(k)}\} \cdot t_k \tag{22}$$

Though both $\{N_t'\}$ and U' appear to be laminate properties, they are functions of the crack densities. Both quantities can be obtained as functions of λ_x and λ_y using the FE analysis. A unit cell is subjected to boundary conditions for zero strains ($\varepsilon_x = 0$ and $\varepsilon_y = 0$) as described in Sec. III. It is then subjected to a temperature change ΔT. Volume averaged stress resultants $\{N\}$ can then be obtained using Eqs. (15) and (16) which is equal to $-\{N_t\}$ [substitute $\varepsilon = 0$ in Eq. (20)]. Dividing $\{N_t\}$ with the imposed temperature load, ΔT, gives $\{N_t'\}$ for that particular combination of λ_x and λ_y. Response surfaces approximations for the two components of $\{N_t'\}$ can be obtained as shown in Figs. 8a and 8b. Analytical expressions can be obtained using least squares polynomial fitting as described in Sec. V (for components of the $[A]$ matrix).

The FE analysis to obtain $\{N_t'\}$ can be used to calculate U' as well. When zero strains, $\{\varepsilon\} = 0$, are imposed on the unit cell in the FE analysis, the first two terms in the parentheses in Eqs. (18) and (19) vanish. Thus, the third term gives the areal strain energy density (strain energy per unit area) of the laminate. From the finite element analysis, the total strain energy of the unit cell can be obtained. This quantity when divided by the volume of the unit cell and ΔT^2 and multiplied by laminate thickness gives U' for that particular combination of λ_x and λ_y. A response surface approximation for U' is shown in Fig. 8c. An analytical expression was obtained by the least squares approximation.

The analytical expressions for components of $[A]$ and $\{N_t'\}$, and U' can be used in Eqs. (18) and (19) to obtain the strain energy for a given temperature change ΔT and applied stress $\{N\}$. Conversely, the stress $\{N\}$ at which the next microcrack forms can be calculated for a given λ_x, λ_y, and ΔT by equating the strain energy difference before and after the formation of the next microcrack to the critical strain energy difference given by Eqs. (5–7). Equations similar to (8–10) can be obtained which include the thermal effects.

The procedure of including the effect of the thermal stresses compared with the uniaxial model of Nairn. The $[90_2/0]$ laminate discussed in Sec. V was used for this purpose. A laminate with a given crack density is subjected to a temperature variation ΔT and is subjected to biaxial stresses N_x and N_y such that $\alpha = 2.0$. The values of N_x or N_y at which the next microcracks form are calculated. Comparison of the predictions has been presented in Table 3. The overall comparison is excellent.

VII. Summary

A novel extension to a methodology proposed by Nairn based on finite fracture mechanics is presented which predicts microcrack densities in symmetric cross-ply laminates subjected to biaxial mechanical and thermal loads. Both load and displacement control conditions were considered. The method was compared to published data.

An FE method was presented to obtain the laminate stiffness matrix $[A]$ of a bidirectionally microcracked laminate with arbitrary crack densities. Approximate analytical expressions for the components of $[A]$ as a function of the two crack densities were derived using the response surface approximation techniques. These analytical expressions were used to predict the progressive bidirectional microcracking of a cross-ply laminate. The procedure was further extended to predict the formation of microcracks due to thermal stresses.

The proposed procedure is limited to cross-ply composites loaded in their principal material directions by a uniform in-plane stress field without shear. Furthermore, crack formation is assumed to occur instantaneously and across the whole width and length of the composite. The current approach should be viewed as an initial contribution to predict progressive bidirectional microcracking in thermomechanically loaded composites.

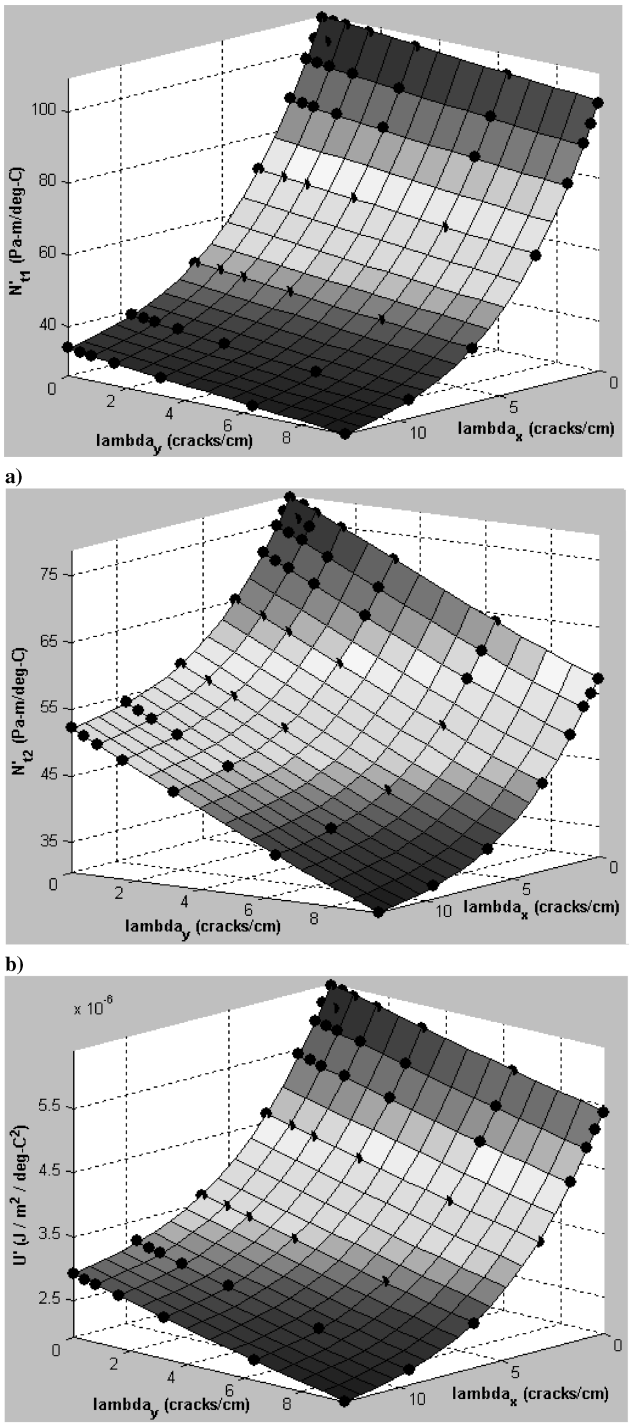

Fig. 8 Fitting complete cubic polynomials with least squares approximation over 56 data points (black dots) obtained from FE simulations. a) N_{t1}', b) N_{t2}', and c) U'.

Appendix

The force resultants are defined as

$$\{N\} = \sum_{k=1}^{NL} \{\sigma^{(k)}\} \cdot t_k \tag{A1}$$

where $\{N\}$ is the 2×1 stress resultant vector, $\{\sigma^{(k)}\}$ is the 2×1 vector of ply stresses in the kth ply, t_k is the thickness of the kth ply, and NL is the number of layers in the laminate. The ply-stress vector can be written in terms of ply stiffness and strains as

Table 3 Comparison of the current model results with Nairn's model for the effect of thermal stresses. A temperature difference value, ΔT, of −280°C was used. σ_x and σ_y are the stresses at which the next microcacks form in the laminate. The directions of the x and y axes can be viewed in Fig. 3

Surface cracks ($\lambda_x = 3.15\ cracks/cm$ *and* $\lambda_y = 0.0\ cracks/cm$)			
Loading condition	σ_x, MPa, [3]	σ_x, MPa, current model	Difference %
Load control	1002	1040	3.8
Internal cracks ($\lambda_x = 0.0\ cracks/cm$ *and* $\lambda_y = 3.15\ cracks/cm$)			
Loading condition	σ_y, MPa, [3]	σ_y, MPa, current model	Difference %
Load control	1091	1143	4.8

$$\{\sigma^{(k)}\} = [\bar{Q}^{(k)}] \cdot (\{\varepsilon\} - \{\alpha^{(k)}\} \cdot \Delta T) \tag{A2}$$

where $[\bar{Q}^{(k)}]$ is the 2×2 stiffness matrix of the kth ply, $\{\varepsilon\}$ is the 2×1 laminate strain vector, $\{\alpha^{(k)}\}$ is the 2×1 vector of CTEs of the kth ply, and ΔT is the temperature difference with reference to the stress free temperature. Substituting Eq. (A2) into Eq. (A1), we obtain

$$\{N\} = [A]\{\varepsilon\} - \{N_t\} \tag{A3}$$

where $[A]$ is the 2×2 laminate stiffness matrix, and the "thermal force" vector $\{N_t\}$ is defined as

$$\{N_t\} = \sum_{k=1}^{NL} [\bar{Q}^{(k)}]\{\alpha^{(k)}\} \cdot t_k \Delta T \tag{A4}$$

The strain energy density in the kth ply is given by

$$U_0^{(k)} = \tfrac{1}{2}\{\sigma^{(k)}\}(\{\varepsilon\} - \{\alpha^{(k)}\} \cdot \Delta T) \tag{A5}$$

Substituting for $\{\sigma^{(k)}\}$ from Eq. (A2) and simplifying, we obtain

$$U_0^{(k)} = \tfrac{1}{2}\{\varepsilon\}^T[\bar{Q}^{(k)}]\{\varepsilon\} - \{\varepsilon\}^T[\bar{Q}^{(k)}]\{\alpha^{(k)}\} \cdot \Delta T + \tfrac{1}{2}\{\alpha^{(k)}\}^T[\bar{Q}^{(k)}]\{\alpha^{(k)}\} \cdot \Delta T^2 \tag{A6}$$

The strain energy density of a unit cell for displacement control conditions is then given by integration of Eq. (A6) over the composite thickness.

$$U = \left(\frac{1}{2}\{\varepsilon\}^T[A]\{\varepsilon\} - \{\varepsilon\}^T\{N_t\} + \sum_{k=1}^{NL}\frac{1}{2}\{\alpha^{(k)}\}^T[\bar{Q}^{(k)}]\{\alpha^{(k)}\} \cdot \Delta T^2 t_k\right) \cdot \frac{1}{\lambda_x} \cdot \frac{1}{\lambda_y} \tag{A7}$$

where λ_x and λ_y are the crack densities defining the unit cell. By substituting for $\{\varepsilon\}$ from Eq. (A2) into Eq. (A7) we get the strain energy in a unit cell for load control conditions.

$$U = \left(\frac{1}{2}\{N\}^T[\bar{A}]\{N\} - \frac{1}{2}\{N_t\}^T[\bar{A}]\{N_t\} + \sum_{k=1}^{NL}\frac{1}{2}\{\alpha^{(k)}\}^T[\bar{Q}^{(k)}]\{\alpha^{(k)}\} \cdot \Delta T^2 t_k\right) \cdot \frac{1}{\lambda_x} \cdot \frac{1}{\lambda_y} \tag{A8}$$

Acknowledgement

This research is supported by the NASA CUIP (formerly URETI) Grant NCC3-994 of the Institute for Future Space Transport (IFST) at the University of Florida. The program manager is Claudia M. Meyer at NASA Glenn Research Center.

References

[1] McCartney, L. N., "Mechanics for the Growth of Bridged Cracks in Composite Materials: Part 1 Basic Principles," *Composites Technology and Research*, Vol. 14, No. 3, 1992, pp. 133–146.

[2] McCartney, L. N., "Mechanics for the Growth of Bridged Cracks in Composite Materials: Part 2 Applications," *Composites Technology and Research*, Vol. 14, No. 3, 1992, pp. 147–154.

[3] Nairn, J. A., "Matrix Microcracking in Composites," *Polymer Matrix Composites*, edited by R. Talreja and J.-A. E. Manson, Vol. 2, Comprehensive Composite Materials, Elsevier Science, New York, 2000, Chap. 13.

[4] Tong, J., Guild, F. J., Ogin, S. L., and Smith, P. A., "On Matrix Crack Growth in Quasi-Isotropic Laminates—1. Experimental Investigation," *Composites Science and Technology*, Vol. 57, No. 11, 1997, pp. 1527–1535.

[5] Tong, J., Guild, F. J., Ogin, S. L., and Smith, P. A., "On Matrix Crack Growth in Quasi-Isotropic Laminates—1. Finite Element Analysis," *Composites Science and Technology*, Vol. 57, No. 11, 1997, pp. 1537–1545.

[6] Varna, J., Joffe, R., Akshantala, N. V., and Talreja, R., "Damage in Composite Lamintes with Off-Axis Plies," *Composites Science and Technology*, Vol. 59, No. 14, 1999, pp. 2139–2147.

[7] McCartney, L. N., and Schoeppner, G. A., "Predicting the Effect of Non-Uniform Ply Cracking on the Thermoelastic Properties of Cross-Ply Laminates," *Composites Science and Technology*, Vol. 62, No. 14, 2002, pp. 1841–1856.

[8] Silberschmidt, V. V., "Matrix Cracking in Cross-Ply Laminates: Effect of Randomness," *Composites Part A: Applied Science and Manufacturing*, Vol. 36, No. 2, 2005, pp. 129–135.

[9] McCartney, L. N., "Predicting Transverse Crack Formation in Cross-Ply Laminates," *Composites Science and Technology*, Vol. 58, No. 7, 1998, pp. 1069–1081.

[10] McCartney, L. N., "Model to Predict Effects of Triaxial Loading on Ply Cracking in General Symmetric Laminates," *Composites Science and Technology*, Vol. 60, No. 12–13, 2000, pp. 2255–2279.

[11] Wang, A. S. D., Chou, P. C., and Lei, S. C., "A Stochastic Model for the Growth of Matrix Cracks in Composite Materials," *Journal of Composite Materials*, Vol. 18, No. 3, 1984, pp. 239–254.

[12] Fukunaga, H., Chou, T. W., Peters, P. W. M., and Schulte, K., "Probabilistic Failure Strength Analysis of Graphite/Epoxy Corss-Ply Laminates," *Journal of Composite Materials*, Vol. 18, No. 4, 1984, pp. 339–356.

[13] Laws, N., and Dvorak, G. J., "Progressive Transverse Cracking in Composite Laminates," *Journal of Composite Materials*, Vol. 22, No. 10, 1988, pp. 900–916.

[14] Berthelot, J.-M., and Le Corre, J.-F., "Statistical Analysis of the Progression of Transverse Cracking and Delamination in Cross-Ply Laminates," *Composites Science and Technology*, Vol. 60, No. 14, 2000, pp. 2659–2669.

[15] Garrett, K. W., and Bailey, J. E., "Multiple Transverse Fracture in 90° Cross-Ply Laminates of a Glass Fibre-Reinforced Polyester," *Journal of Material Science*, Vol. 12, No. 1, 1977, pp. 157–168.

[16] Crossman, F. W., Warren, W. J., Wang, A. S. D., and Law, G. E., Jr., "Initiation and Growth of Transverse Cracks and Edge Delamination in Composite Laminates: Part 2. Experimental Correlation," *Journal of Composite Materials Supplement*, Vol. 14, No. 1, 1980, pp. 89–108.

[17] Lee, J. W., and Daniel, I. M., "Progressive Transverse Cracking of Crossply Composite Laminates," *Journal of Composite Materials*, Vol. 24, Nov. 1990, pp. 1225–1243.

[18] Lim, S. G., and Hong, C. S., "Effect of Transverse Cracks on the Thermomechanical Properties of Cross-Ply Laminated Composites," *Composites Science and Technology*, Vol. 34, No. 2, 1989, pp. 145–162.

[19] Zhang, J., Fan, J., and Soutis, C., "Analysis of Multiple Matrix Cracking in $[\pm\theta m/90n]s$ Composite Laminates. Part 1: In-Plane Stiffness Properties," *Composites*, Vol. 23, No. 5, 1992, pp. 291–298.

[20] Berthelot, J. M., Leblond, P., El Mahi, A., and Le Corre, J. F., "Transverse Cracking of Cross-Ply Laminates: Part 1. Analysis," *Composites Part A*, Vol. 27A, No. 10, 1996, pp. 989–1001.

[21] Hashin, Z., "Analysis of Stiffness Reduction of Cracked Cross-Ply Laminates," *Engineering Fracture Mechanics*, Vol. 25, No. 5/6, 1986, pp. 771–778.

[22] Nairn, J. A., "The Strain Energy Release Rate of Composite Microcracking: A Variational Approach," *Journal of Composite Materials*, Vol. 23, Nov. 1989, pp. 1106–1129.

[23] Nairn, J. A., "Some New Variational Mechanics Results on Composite Microcracking," *Proceedings of ICCM-10*, Woodhead Publishing Ltd., Cambridge, U.K., Aug. 1995.

[24] Varna, J., Berglund, L. A., Talreja, R., and Jakovics, A., "A Study of the Opening Displacement of Transverse Cracks in Cross-Ply Laminates," *International Journal of Damage Mechanics*, Vol. 2, July 1993, pp. 272–289.

[25] Varna, J., Berglund, L. A., Krasnikovs, A., and Chihalenko, A., "Crack Opening Geometry in Cracked Composite Laminates," *International Journal of Damage Mechanics*, Vol. 6, Jan. 1997, pp. 96–118.

[26] Varna, J., Akshantala, N. V., and Talreja, R., "Crack Opening Displacement and the Associated Response of Laminates with Varying Constraints," *International Journal of Damage Mechanics*, Vol. 8, April 1999, pp. 174–193.

[27] Joffe, R., and Varna, J., "Analytical Modeling of Stiffness Reduction in Symmetric and Balanced Laminates due to Cracks in 90° Layers," *Composites Science and Technology*, Vol. 59, No. 11, 1999, pp. 1641–1652.

[28] Qu, J., and Hoiseth, K., "Evolution of Transverse Matrix Cracking in Cross-Ply Laminates," *Fatigue & Fracture of Engineering Materials & Structures*, Vol. 21, No. 4, 1998, pp. 451–464.

[29] Berthelot, J.-M., "Transverse Cracking and Delamination in Cross-Ply Glass-Fiber and Carbon-Fiber Reinforced Plastic Laminates: Static and Fatigue Loading," *Applied Mechanics Reviews*, Vol. 56, No. 1, 2003, pp. 111–147.

[30] Aboudi, J., Lee, S. W., and Herakovich, C. T., "Three-Dimensional Analysis of Laminates with Cross Cracks," *Journal of Applied Mechanics*, Vol. 55, No. 2, 1988, pp. 389–397.

[31] Herakovich, C. T., and Hyer, M. W., "Damage-Induced Property Changes in Composites Subjected to Cyclic Thermal Loading," *Engineering Fracture Mechanics*, Vol. 25, No. 5/6, 1986, pp. 779–791.

[32] Timmerman, J. F., and Seferis, J. C., "Predictive Modeling of Microcraking in Carbon-Fiber/Epoxy Composites at Cryogenic Temperatures," *Journal of Applied Polymer Science*, Vol. 91, No. 2, 2004, pp. 1104–1110.

[33] McManus, H. L., and Maddocks, J. R., "On Microcracking in Composite Laminates Under Thermal and Mechanical Loading," *Polymer & Polymer Composites*, Vol. 4, No. 5, 1996, pp. 305–314.

[34] Park, C. H., and McManus, H. L., "Thermally Induced Damage in Composite Laminates: Predictive Methodology and Experimental Investigation," *Composites Science and Technology*, Vol. 56, No. 10, 1996, pp. 1209–1219.

A. Roy
Associate Editor